Available online at www.sciencedirect.com
ScienceDirect
Journal of Power Sources 159 (2006) 1034–1041
JOURNAL OF POWER SOURCES
www.elsevier.com/locate/jpowsour

Link-up of a bench-scale "shift-less" gasoline fuel processor to a polymer electrolyte fuel cell

M. Bosco [a], F. Hajbolouri [b], T.-B. Truong [a], E. De Boni [a], F. Vogel [a,*], G.G. Scherer [b]

[a] *Laboratory for Energy and Materials Cycles (LEM), General Energy Department, Paul Scherrer Institut, 5232 Villigen-PSI, Switzerland*
[b] *Electrochemistry Laboratory (ECL), General Energy Department, Paul Scherrer Institut, 5232 Villigen-PSI, Switzerland*

Received 18 July 2005; received in revised form 1 December 2005; accepted 12 December 2005
Available online 9 February 2006

Abstract

The rapid development of the polymer electrolyte fuel cell (PEFC) technology in recent years has stimulated research in all areas of fuel processing catalysis for hydrogen generation. A new precious metal catalyst with an improved precious metal utilisation, which allows the low temperature reforming (550–650 °C) of hydrocarbons, was developed. The low temperature reforming results in low carbon monoxide concentrations, in the range of 2–5 vol.%, making it possible to omit the shift units before the preferential oxidation unit (PROX). For the PROX unit a selective catalyst was developed to oxidize the carbon monoxide down to a level acceptable for PEFCs.

To demonstrate the "shift-less" fuel processing concept, a test unit was built containing a gasoline reformer and a PROX unit. At GHSV of 3319–19795 h^{-1} and $T = 595$–645 °C complete conversion of C_{2+} was achieved. First, a dual fixed-bed reactor configuration with staged air supply was tested for the PROX. With this configuration hot spots over 280 °C occurred, which made a selective conversion of carbon monoxide impossible. The hot-spot problem was drastically reduced by using an annulus reactor achieving >99.93% carbon monoxide conversion due to the better heat dissipation. The hydrogen conversion in the PROX unit was high at around 27%. This value may be improved by better temperature control of the PROX reactor. Reformate gas with hydrogen concentrations up to 51 vol.% could be produced from sulphur-free gasoline (RON = 95). Reformate gas with 32% H_2 and <36 ppmv CO was fed to a 30 cm^2 polymer electrolyte fuel cell. A stable cell voltage of 680 mV was obtained at a current density of 500 mA cm^{-2} for operation with pure O_2 as oxidant. Changing the oxidant to air led to a cell voltage decline of 120 mV.

Keywords: Hydrogen; Fuel processing; Gasoline reforming; Low temperature reforming; Polymer electrolyte fuel cell

1. Introduction

Hydrogen is the fuel of choice for polymer electrolyte fuel cells. For mobile applications there are some major unresolved issues, like the missing fuel infrastructure. This makes on-board fuel processors with liquid fuels attractive for producing hydrogen for fuel cells [1,2]. Gasoline reforming provides a method to produce hydrogen for fuel cells in mobile applications [3–6]. The gasoline distribution system is already in place. Mizsey [7] compared different vehicle power trains. A gasoline reformer–fuel cell power train reached a "Well-to-Wheel" efficiency of 25%, compared to 18% for an ICE. By comparing the different fuels [8] for fuel cells (FC), advantages and disadvantages can be seen. FC-systems driven with pure hydrogen have the best efficiency, as during reforming of methanol or gasoline a part of the energy in the fuel is used for reforming. On the other hand, the hydrogen storage needs additional space, due to the low volumetric energy density of hydrogen. Another drawback of pure hydrogen as fuel is the absence of a hydrogen distribution infrastructure. Methanol is a liquid and can easily be used like gasoline. From a technical point of view, it is easier and more efficient to reform methanol than gasoline. The drawback is, as for pure hydrogen, the absence of a distribution infrastructure. The better "Tank-to-Wheel" efficiencies of pure hydrogen and methanol decrease by looking at the "Well-to-Wheel" efficiency. The production of gasoline and diesel from crude oil is more efficient than the production of hydrogen and methanol from natural gas.

There are problems for fuel processors [9] which have to be solved, like the interfaces between the fuel processor and the peripheral components (pump and flow control), the interface between the fuel processor and the fuel cell stack, and control issues.

* Corresponding author. Tel.: +41 56 310 21 35; fax: +41 56 310 21 99.
E-mail address: frederic.vogel@psi.ch (F. Vogel).

0378-7753/$ – see front matter © 2005 Elsevier B.V. All rights reserved.
doi:10.1016/j.jpowsour.2005.12.025

Nomenclature

ATR	autothermal reforming
BET	method to measure surface area by physisorption
C_{2+}	hydrocarbons with two and more carbon atoms
FID	flame ionization detector
GC	gas chromatograph
GHSV	gas hourly space velocity ($Nl\,h^{-1}\,l_{cat.}{}^{-1}$)
ICE	internal combustion engine
LHV	lower heating value
O/C	oxygen-to-carbon ratio (mol/mol)
PEFC	proton exchange membrane fuel cell
POX	partial oxidation
PROX	preferential oxidation
RON	research octane number
S/C	steam-to-carbon ratio (mol/mol)
TCD	thermal conductivity detector
WHSV	hydrocarbon weight hourly space velocity ($g_{HC}\,h^{-1}\,g_{cat.}{}^{-1}$)

The route of choice for mobile applications is autothermal reforming [10,11], because it allows for fast start-up and high reformer efficiencies [12–14]. Fig. 1 depicts the process steps necessary to produce PEFC-grade hydrogen from gasoline.

The stoichiometry for the reaction of gasoline with air and water may be written as:

$$C_{7.3}H_{12.6} + nO_2 + (14.6 - 2n)H_2O + 4nN_2 \rightarrow (20.9 - 2n)H_2 + 7.3\,CO_2 + 4nN_2 \quad (1)$$

Depending on the application, gasoline may be reacted with water only (steam reforming, $n = 0$), with air only (partial oxidation, $n = 7.3$), or with a mixture of air and water (autothermal reforming, $n = 3$). For low temperature reforming ($T < 700\,^{\circ}C$) Eq. (1) is a good approximation for the product distribution. For higher temperatures a significant amount of CO will be formed.

Most developments focus on high temperature reforming followed by high temperature and low temperature shift reactors to reduce the CO content and to produce more hydrogen [4,6,12]. Final CO cleanup is achieved in a preferential oxidation reactor [15], where CO is oxidized to CO_2. Other developments try to integrate all steps in one reactor [10], the achievable hydrocarbon conversion was over 90%. PSI's "shift-less" concept operates at lower temperatures in the reformer, but using more water than would be required for autothermal reforming according to Eq. (1), producing much less CO, and is thus able to omit the shift reactors. The challenges are:

- To find a catalyst active for gasoline reforming at lower temperatures, producing high yields of hydrogen.
- To reduce the CO content from 5% to less than 50 ppmv (>99.9% conversion) without loosing much hydrogen.

Preliminary "tank-to-electricity" calculations yielded a maximum efficiency of 33% (LHV) for the "shift-less" concept, assuming a hydrogen utilization of 85% and a fuel cell efficiency of 50% [16]. This number compares well with the conventional route including two shift reactors [3]. The main benefit of the "shift-less" concept is the much simpler design with only two instead of four catalytic reactors, leading to faster start-up and response times and smaller system volumes [17,18].

To demonstrate the technical feasibility of PSI's "shift-less" concept, a lab-scale fuel processor and a link up to a PEFC was built. The goals were:

- To produce a hydrogen-rich reformate gas with <50 ppm of CO from sulfur-free gasoline.
- To study the influences of using such a real reformate gas on the performance of a PEFC.

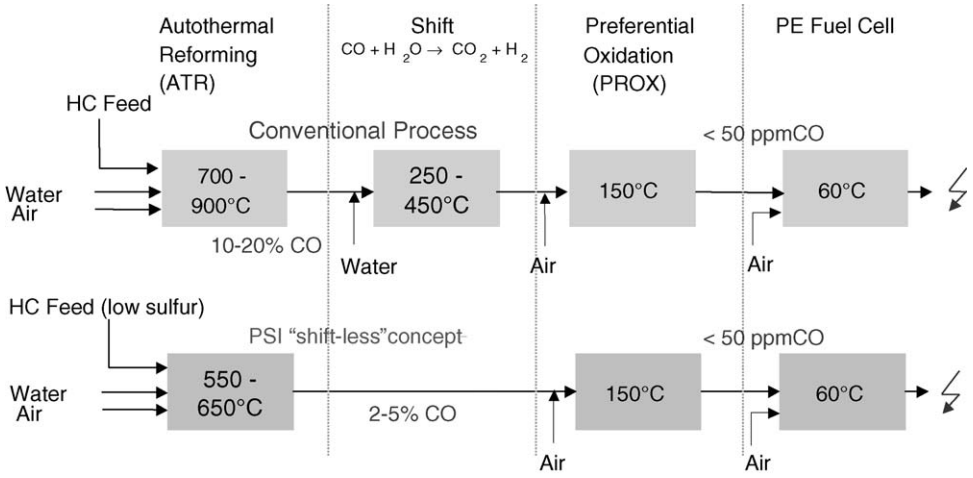

Fig. 1. Main steps in the reforming of gasoline for producing fuel cell-grade hydrogen. Top: state-of-the art process including autothermal reforming, one or two shift reactors, a preferential CO oxidation unit, and the PEFC. Bottom: PSI's "shift-less" concept operates at lower temperatures in the reformer, producing much less CO, and is thus able to omit the shift reactors.

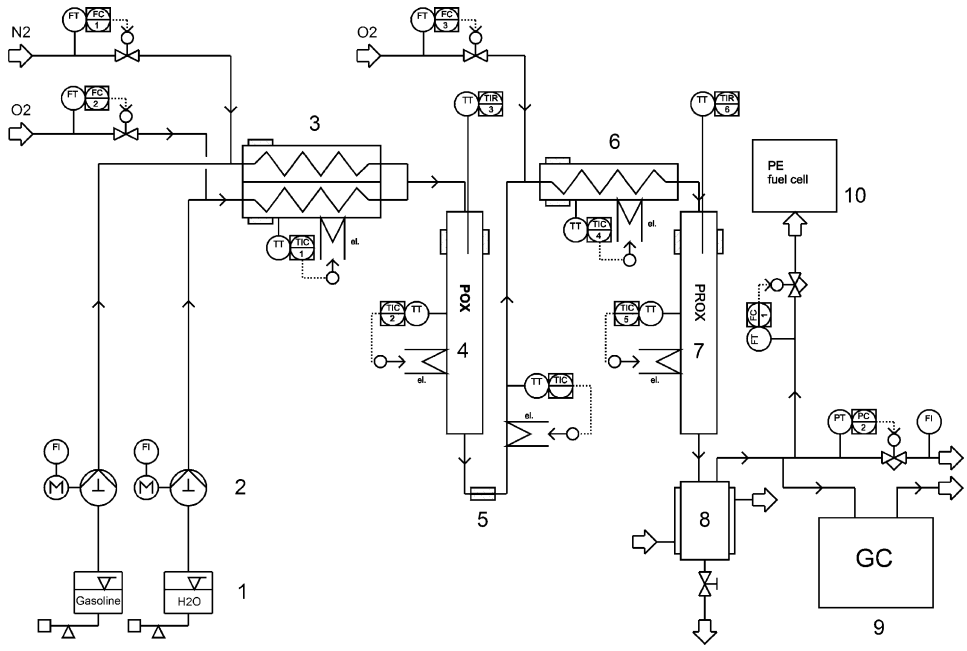

Fig. 2. Flowchart of fuel processing unit. (1) Balances for water and gasoline, (2) HPLC pumps, (3) evaporators and superheaters, (4) POX reactor with moveable thermocouple in thermowell, (5) heated transfer line, (6) heater, (7) PROX reactor, (8) water cooled condenser, (9) gas chromatograph with TCD and FID detectors, (10) PE fuel cell (including humidification).

2. Experimental

Building on earlier results from methanol and hydrocarbon reforming [3,19,20], a continuous fixed-bed fuel processor, consisting of a catalytic partial oxidation (POX) reactor and a preferential oxidation (PROX) reactor was built. Fig. 2 shows the flowchart of the fuel processing unit. Water and gasoline (isomerate–platformate mixture 48:52 wt.%, RON = 95, $S < 1$ ppm) were pumped as liquids, vaporized and mixed with air, before entering the POX reactor (I.D. = 16 mm, $L = 482$ mm). In the top section of the reactor, 1 g of a proprietary 1% Rh/5% Ce–ZrO_2 powder catalyst [3] (particle size range 250–500 μm, BET = 58 $m^2\,g^{-1}$, dispersion = 94%) was diluted with 12 g of quartz sand. In the main section of the POX reactor, 15 g of the same powder catalyst were diluted with 60 g of quartz sand.

The reformate gas was fed to the PROX reactor via a heated transfer line. Just before entering the PROX reactor it was mixed with oxygen. The PROX reactor (Fig. 3) was of an annular type (annular gap = 2.75 mm, $L = 200$ mm), which facilitates the heat dissipation. Preliminary experiments with a dual fixed-bed reactor configuration with staged air supply generated hot spots of over 280 °C, which made a selective CO conversion impossible. In the top section of the bed 1 g of a proprietary 5%Ru/5%Ce–γ-Al_2O_3 powder catalyst (particle size range 125–250 μm, BET = 165 $m^2\,g^{-1}$, dispersion = 8.1%) was diluted with 20 g of quartz sand. In the main section of the PROX reactor, 5 g of the same powder catalyst was diluted with 20 g of quartz sand. The different catalyst dilution ratios avoided extreme hot spots in the inlet sections of the reactors. Both POX and PROX reactors were heated electrically for start-up and to compensate for heat losses during operation. Movable thermocouples in thermowells were placed in both reactors to measure the temperature profile in the catalyst bed during reaction. Fig. 4 shows a picture of the lab-scale fuel processing unit.

The gas composition was analyzed on-line for CH_4, CO_2, CO, H_2, O_2, N_2 on an HP 6890 GC using a TCD and a two-column switching system with helium as the carrier gas. Unreacted hydrocarbons in the reformate gas were analyzed on the same GC with an FID. Total volumetric flow of reformate was determined by a wet test meter. Fuel processor control and data acquisition were performed by a LabView™ program.

After the PROX the reformate gas was fed to a water cooled condenser, to remove the excess water. The condenser was also used as liquid trap in case of incomplete conversion of gasoline, but could be omitted in an improved design. Then the reformate gas was fed through a humidifier to the fuel cell.

Fig. 3. Top view of annular type PROX reactor.

Fig. 4. Lab-scale gasoline fuel processor consisting of an autothermal reformer and a preferential oxidation reactor.

All the fuel cell measurements were performed in a 30 cm^2 test cell with meander flow field graphite plates. A catalyst coated membrane (PtRu on anode and Pt on cathode) and two different gas diffusion layers were used as membrane electrode assembly (MEA). The measurements were performed in a cell temperature range of 60–80 °C. Both the fuel and the oxidant were fed with an excess of 50% to the stoichiometric requirements and were humidified at 35 °C. When air was used as oxidant the cathode inlet was humidified at 55 °C. The steady state current–voltage curves were recorded manually [21,22].

3. Results and discussion

First experiments were performed to maximize hydrogen and minimize methane concentration in the reformate gas (experiments A and B). The process parameters T (reformer outlet temperature), WHSV (hydrocarbon weight hourly space velocity), and S/C (steam-to-carbon molar ratio) were varied, whereas the O/C ratio was kept constant at 0.5. Best conditions for maximum hydrogen concentration were found in experiment A/3 (see Table 1). The high reformate gas flow in experiments A and B produced hot spots up to 228 °C in the PROX unit, and the CO concentration at the PROX outlet could not be reduced to a level low enough for the PEFC. For this reason we chose to reduce the gasoline feed flow to the PROX reactor (experiments C–F). A second series of experiments was performed to minimize the CO

Table 1
Operating conditions of POX and PROX reactors with corresponding dry gas results

Experiment	POX conditions					PROX conditions			Dry gas after PROX					
	S/C	O/C	WHSV (h^{-1})	GHSV (h^{-1})	T_{outlet} (°C)	$O^{in}_{2,PROX}$ (ml min^{-1})	GHSV (h^{-1})	$T_{hotspot}$ (°C)	H_2 (vol.%)	CO (vol.%)	CO_2 (vol.%)	CH_4 (vol.%)	N_2 (vol.%)	Reformate (l/h)
A/1	2.6	0.5	1.1	3319	630	0	–	–	43.7	6.5	18.7	7.3	25.1	93.7
A/2	2.6	0.5	1.6	13978	645	0	–	–	45.7	7	18.1	5.9	24.9	146.5
A/3	4.2	0.5	1.6	19795	637	0	–	–	51.2	5	19.3	3.4	21.8	157.3
A/4	4.2	0.5	1.6	19795	637	74	34163	215	48.5	0.4	25.0	3.8	22.7	150.7
B/1	4.2	0.5	1.6	19795	637	114	34612	220	49.3	0.46	25.6	4.0	23.6	152.1
B/2	4.2	0.5	1.6	19795	637	150	35067	228	47.9	0.39	26.2	4.3	24.2	154.2
C*	3.6	0.7	0.4	4972	545	23	13290	164	27.9	0.000	25.4	10.9	37.8	30.7
D*	2.6	0.5	0.7	5870	610	45	17373	142	21.0	0.054	27.8	19.2	31.7	32.6
E*	3.0	0.6	0.4	4654	585	37	11544	168	27.9	0.003	27.9	9.3	35.8	33.4
F*	2.6	0.5	0.5	4659	595	46	12634	188	31.7	<0.004	28.8	13.2	27.0	35.8

Pressure = 4 bar, conversion C_{2+} = 100% for all experiments.
* Measured gas concentration during link-up with fuel cell.

Table 2
Results (after PROX) and comparisons to theory from different experiments

Experiment	H_2 flow (l/h)	H_2 Yield (mol H_2/mol $C_{7.3}H_{12.6}$)	H_2 yield % stoichiometry[a]	H_2O% excess[b]
A/1	41	9.5	54.0	61.1
A/2	67	10.3	58.8	61.0
A/3	81	12.4	70.8	160.5
A/4	73	11.3	64.2	160.5
B/1	75	11.6	65.9	160.5
B/2	82	12.7	72.3	160.5
C	9	5.3	32.9	157.8
D	7	2.5	14.5	61.6
E	9	5.4	33.0	111.0
F	11	5.3	29.9	60.7

[a] The oxygen feed in the experiments is used to calculate n in the proposed stoichiometry (Eq. (1)). The theoretically produced hydrogen is compared to the effective produced hydrogen in the experiment.

[b] The proposed stoichiometry (Eq. (1)) is used together with the factor *n* (calculated from the oxygen used in the experiment). The water excess is calculated by comparing the theoretical value (with factor *n*) and the effective feed of water.

concentration in the reformate gas stream (experiments C–F). Now the hot spot could be kept below 190 °C. The best conditions for minimizing the CO concentration after the PROX unit are summarized in Tables 1 and 2.

In experiment A/1 → A/2 the WHSV was varied from 1.1 to 1.6 h^{-1}. The reformate gas composition did not change significantly (Fig. 5), but in the temperature profile a significant shift of the maximal temperature towards the end of the catalyst bed occurred (Fig. 6). In a next step the S/C parameter was increased from 2.6 to 4.2 (A/2 → A/3). More hydrogen and less methane and CO was produced (Fig. 5). The temperature profile had the same shape but the mean temperature was a bit lower than in experiment A/1, probably due to the increased steam reforming (Fig. 6). At 17:00 h, oxygen was fed to the PROX reactor, but the CO concentration could not be reduced below 1 vol.% due to the temperature of more than 210 °C in the PROX reactor (Fig. 7). For experiments B, the POX parameters were set the same as at the end of experiment A/4, and thus the temperature profile for the POX reactor was the same as for experiment A/4 and A/3. The difference to experiments A/3–A/4 was the oxygen flow to the PROX reactor. At the beginning, 114 ml min^{-1} then at 16:30 150 ml min^{-1} were fed. Fig. 7 shows the temperature profile of the PROX reactor. Excessive hot spots up to 228 °C

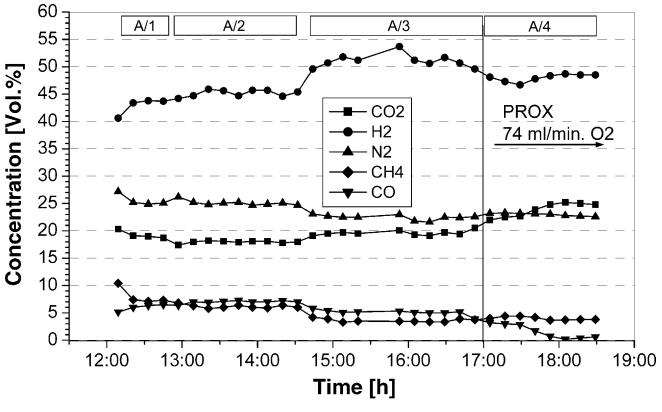

Fig. 5. Reformate gas concentrations (experiments A/1–A/4). A/1: 12:10–12:50 h, A/2: 12:52–14:30 h, A/3: 14:42–17:00 h, A/4: 17:00–18:30 h.

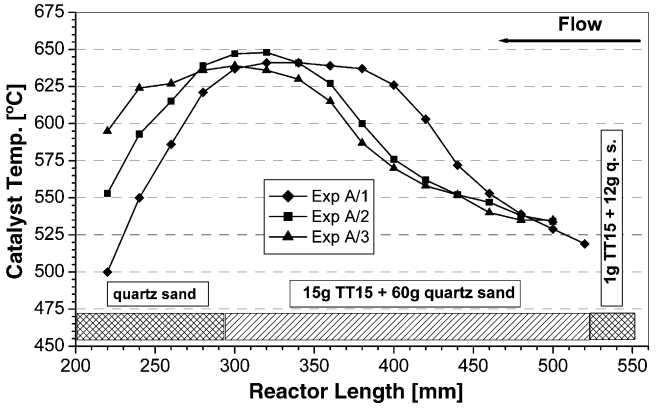

Fig. 6. Temperature profiles in the POX reactor (experiments A/1–A/3).

were measured. To actively cool the PROX reactor, the insulation jacket of the reactor was removed, and air cooling for the inner part of the annulus reactor was installed. The slow response time (12 min) of the GC made a fast control impossible. Fig. 8 shows an unstable CO concentration in the reformate gas. The additional cooling attempts led to unstable PROX conditions. This was mainly due to the manual adjustment of the cooling air flow, guided by the results of the gas analysis and by the ther-

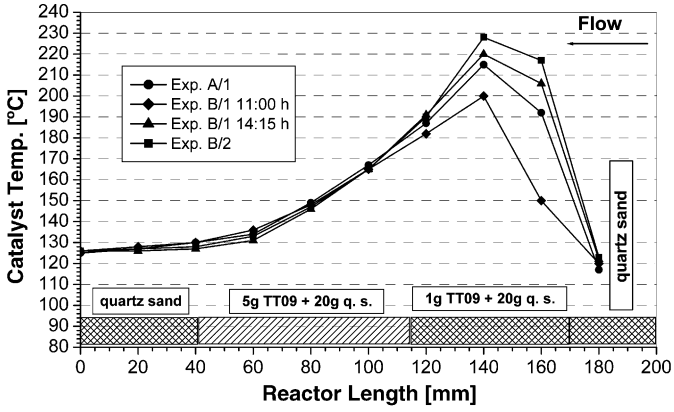

Fig. 7. Temperature profiles in the PROX reactor (experiments A/1, B).

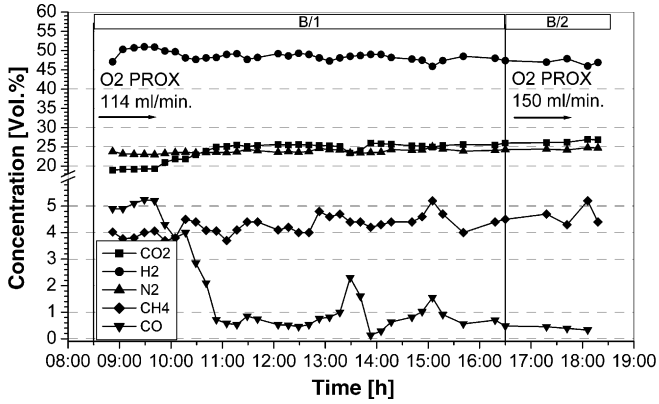

Fig. 8. Reformate gas concentrations (experiments B/1–B/2) B/1: 8:30–16:30 h, B/2: 16:30–18:30 h.

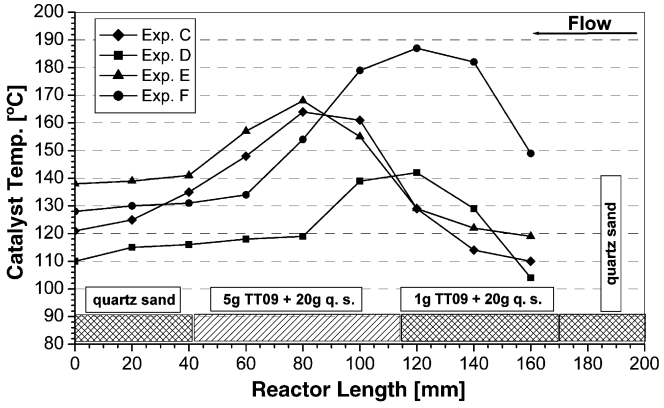

Fig. 10. Temperature profile in the PROX reactor (experiments C–F).

mocouple reading of the hot spot location. Fig. 7 shows hotspots in the PROX reactor up to 230 °C which lead to a preferential oxidation of H_2 and not CO. The CO concentration was reduced to 0.5 vol.%, still hundred times higher than the target value of 50 ppm, and thus link-up to the fuel cell was not attempted.

Experiments C, D, E and F represent successful link-ups to the fuel cell. Fig. 9 shows the measured temperature profiles in the POX reactor during experiments C–F. The CO concentration in the reformate gas could be reduced to an admissible value. In experiments C, E and F the GHSV in the POX reactor was reduced to a quarter of the value used in experiments A and B. The temperature in the PROX reactor (Fig. 10) was low enough to selectively oxidise CO to very low values (Figs. 11–14). The CO levels were now low enough to feed the reformate gas after the condenser directly to the fuel cell.

Best operation conditions were found in experiment F. The hot spot in the PROX reactor increased to 188 °C due to the higher oxygen flow rate. Nevertheless, the CO concentration was reduced below the detection limit of our analysis method, i.e. 36 ppmv. However, 27% of the hydrogen was converted to water. This dry reformate gas was directed to the PEFC. The fuel processor and the fuel cell were operated for 2 h at stable conditions. Fig. 14 shows the composition of the dry reformate gas during experiment F (see Table 2). For this gas composition (experiment F), a stable cell voltage was obtained and the cell

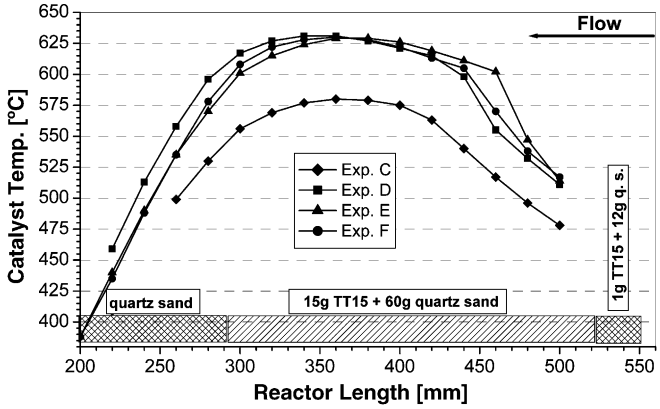

Fig. 9. Temperature profile in the POX reactor (experiments C–F).

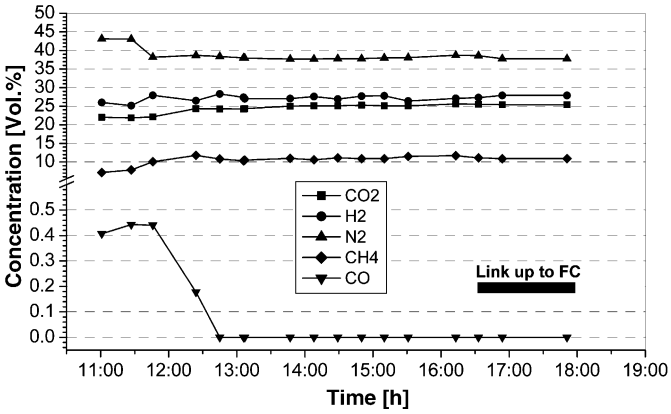

Fig. 11. Dry reformate gas concentrations during link up with PE fuel cell (experiment C) WHSV = 0.4 h^{-1}; GHSV = 4972 h^{-1}; S/C = 3.6; O/C = 0.7; O_2 (PROX) = 144 ml/min.

voltage declined slightly, 40 mV, compared to the cell operation with pure hydrogen (see Fig. 15).

The polarization curves when reformate composition (F) was used as fuel are depicted in Fig. 16. They were recorded manually after operating the cell a couple of hours under steady state conditions. The cell performance proved to be excellent for the operation with reformate as fuel and O_2 as oxidant. A

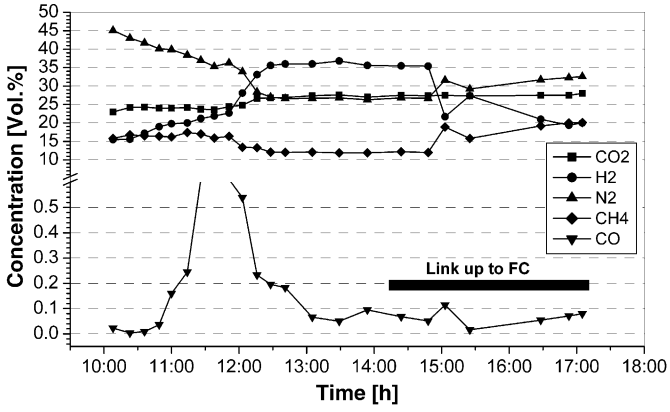

Fig. 12. Dry reformate gas concentrations during link up with PE fuel cell (experiment D) WHSV = 0.7 h^{-1}; GHSV = 5870 h^{-1}; S/C = 2.6; O/C = 0.5; O_2 (PROX) = 45 ml/min.

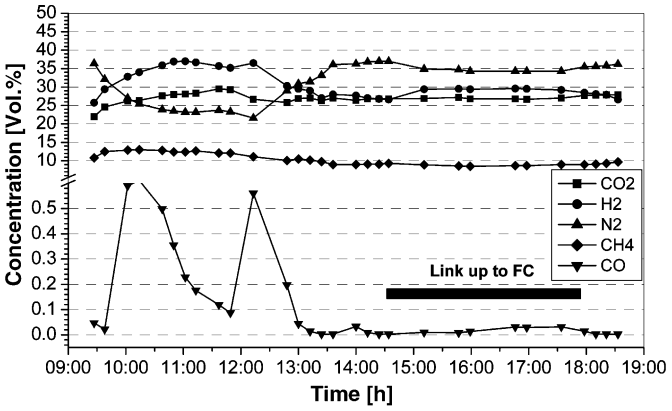

Fig. 13. Dry reformate gas concentrations during link up with PE fuel cell (experiment E) WHSV = 0.4 h^{-1}; GHSV = 4654 h^{-1}; S/C = 3.0; O/C = 0.6; O_2 (PROX) = 37 ml/min.

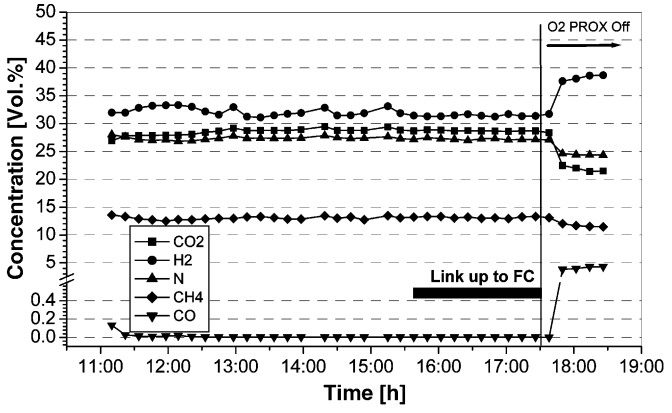

Fig. 14. Dry reformate gas concentrations during link up with PEM fuel cell (experiment F) WHSV = 0.5 h^{-1}; GHSV = 4659 h^{-1}; S/C = 2.6; O/C = 0.5; O_2 (PROX) = 46 ml/min.

cell voltage of 680 mV was obtained at a current density of 500 mA cm^{-2}. Changing the oxidant to air led to a cell voltage decline of 120 mV.

The fuel cell polarization curves for the reformate gas and H_2/100 ppm CO measured under the same operation conditions

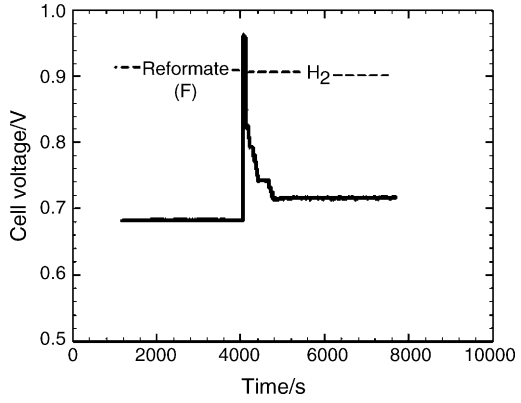

Fig. 15. The cell voltage at 500 mA cm^{-2}. T_{cell} = 60 °C. Reformate or H_2 was used as fuel and O_2 as oxidant. $T_{hum,cathode}$ = 35 °C, $T_{hum,anode}$ = 35 °C. λ_{fuel} = 1.5 and $\lambda_{oxidant}$ = 1.5. $P_{anode} = P_{cathode}$ = 1 bar_a. The composition of the reformate gas is compiled in Table 2.

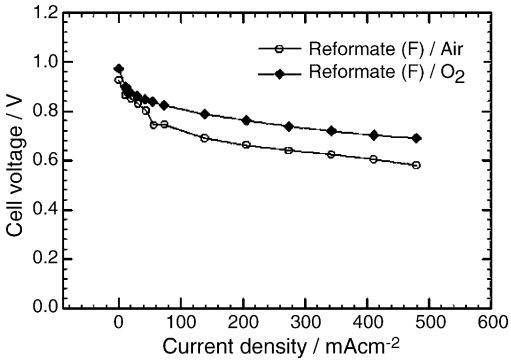

Fig. 16. Polarization curves when reformate gas composition (F) was used as fuel and O_2 or air was used as oxidant. T_{cell} = 60 °C, $T_{hum,cathode}$ = 35 °C, $T_{hum,anode}$ = 35 °C, λ_{fuel} = 1.5, λ_{O_2} = 1.5, and λ_{air} = 2. $P_{anode} = P_{cathode}$ = 1 bar_a.

are compared in Fig. 17. Only a slight performance degradation was recognized for the reformate fuel compared to H_2/100 ppm CO which might be due to the by-products, CO_2, N_2, and CH_4, present in the reformate.

The reformate from experiment F with CO < 36 ppmv was fed to the fuel cell for 2 h. At 17:30 the PEFC was disconnected from the fuel processor, and the oxygen feed to the PROX reactor was switched off. After switching off the oxygen, the hydrogen concentration increased. The increment corresponded to the hydrogen that was oxidized before in the PROX reactor (27%). The total time on stream of the fuel processor was approximately 140 h. No signs of catalyst deactivation were observed.

An interesting aspect of the two sets of experiments A, B and C–F was the methane concentration in the reformate gas stream. In experiments A and B, the methane concentration was 3.4–7.3 vol.%, in experiments C–F, 9.3–19.2 vol.%. The main difference in experiments C–F was the lower WHSV (0.4–0.7 h^{-1}, as opposed to 1.1–1.6 h^{-1} in experiments A and B), leading to longer residence times in the POX reactor. Assuming methane formation by methanation only, a longer residence time, together with the high CO_2 and H_2 concentrations, probably favored the methanation of CO_2:

$$CO_2 + 4H_2 \rightarrow CH_4 + 2H_2O \quad (2)$$

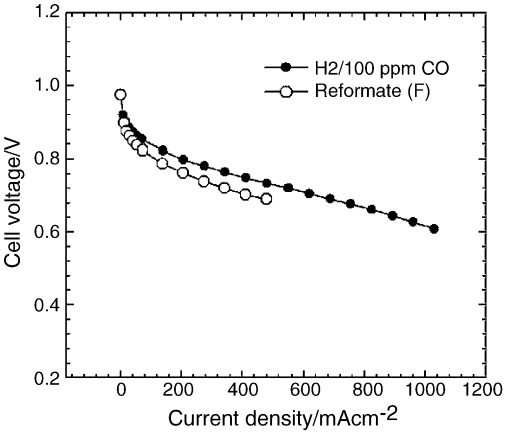

Fig. 17. Comparison of the cell performance for H_2/100 ppm CO and the reformate composition (F). O_2 was used as oxidant. T_{cell} = 60 °C. $T_{hum,cathode}$ = 35 °C, $T_{hum,anode}$ = 35 °C. $\lambda_{fuel} = \lambda_{oxidant}$ = 1.5, $P_{anode} = P_{cathode}$ = 1 bar.

Thus, lowering the WHSV increased the residence time and favored the formation of methane. Methane formation according to Eq. (2) is an undesired reaction because 4 moles of hydrogen are "lost". This is a challenge for the reactor design. Usually, a reformer will be designed for the highest hydrogen output flow expected plus some safety margin. This will lead to longer residence times at lower throughputs and hence lead to a higher concentration of methane at the reactor outlet.

4. Conclusions

Reforming gasoline at temperatures in the range of 550–650 °C using a proprietary noble metal catalyst resulted in lower CO concentrations (4–5%) than conventional reformers. The residence time in the POX reactor had an influence on the methane concentration at the outlet, probably due to the methanation of CO_2. The CO content in the hydrogen-rich reformate could be reduced to <36 ppmv in one PROX reactor. An annular fixed-bed design of the PROX reactor performed much better than a tubular fixed-bed. The limiting factor for achieving higher hydrogen production rates was the heat removal in the PROX reactor, leading to a significant loss of hydrogen (27%). A plate reactor/heat exchanger design may overcome the current limitations.

PSI's "shift-less" fuel processor was successfully linked to a PE fuel cell. The cell performance proved to be excellent for the operation with reformate as fuel and O_2 as oxidant. A cell voltage of 680 mV was obtained at a current density of 500 mA cm^{-2}.

Acknowledgements

The authors thank P. Binkert, P. Hottinger, T. Marti and C. Marmy for assisting the design and setting up of the experimental rig.

References

[1] A.P. Meyer, M.E. Gorman, D.M. Flanagan, D.R. Boudreau, SAE, 2001-01-0540.
[2] W.L. Mitchell, M. Hagan, S.K. Prabhu, SAE, 1999-01-0535.
[3] E. Newson, T.-B. Truong, Int. J. Hydrogen Energy 28 (2003) 1379–1386.
[4] S. Ahmed, M. Krumpelt, Int. J. Hydrogen Energy 26 (2001) 291–301.
[5] D.L. Trimm, A.A. Adesina, M. Praharso, N.W. Cant, Catal. Today 93–95 (2004) 17–22.
[6] A.K. Avci, Z.I. Önsan, D.L. Trimm, Appl. Catal. A: General 216 (2001) 243–256.
[7] P. Mizsey, E. Newson, J. Power Sources 102 (2001) 205–209.
[8] A. Docter, G. Konrad, A. Lamm, VDI 1565 (2000).
[9] D.Z. Megede, J. Power Sources 106 (2002) 35–41.
[10] J.W. Jenkins, E. Shutt, Platinum Metals Rev. 33 (3) (1989) 118–127.
[11] A. Qi, S. Wang, G. Fu, C. Ni, D. Wu, Appl. Catal. A: General 281 (2005) 233–246.
[12] S. Springmann, G. Friedrich, M. Himmen, M. Sommer, G. Eigenberger, Appl. Catal. A General 235 (2002) 101–111.
[13] M. Pacheco, J. Sira, J. Kopasz, Appl. Catal. A General 250 (2003) 161–175.
[14] L. Ma, D.L. Trimm, C. Jiang, Appl. Catal. A General 138 (1996) 275–283.
[15] K.A. Starz, E. Auer, F. Baumann, T. Lehmann, S. Wieland, R. Zuber, SAE, 2000-01-0013.
[16] T. Böhme, Institut für Mess- und Regeltechnik, ETHZ, personal communication, 2003.
[17] M. Castaldi, M. Lyubovsky, R. LaPierre, W.C. Pfefferle, S. Roychoudhury, SAE, 2003-01-1366.
[18] S.G. Goebel, D.P. Miller, W.H. Petti, M.D. Cartwright, Int. J. of Hydrogen Energy 30 (2005) 953–962.
[19] K. Geissler, E. Newson, F. Vogel, T.-B. Truong, P. Hottinger, A. Wokaun, Phys. Chem. Chem. Phys. 3 (2001) 289–293.
[20] P. Mizsey, E. Newson, T.-B. Truong, P. Hottinger, Appl. Catal. A: General 213 (2001) 233–237.
[21] F. Hajbolouri, G.G. Scherer, A. Wokaun, PSI Scientific Report 2003. V 117 (2004). ISSN 1423–7342.
[22] F. Hajbolouri, Diss. ETHZ No. 15525.